Anharmonic contribution to the Debye-Waller factor for copper, silver, and lead

J.T. Day and J.G. Mullen
Physics Department, Purdue University, West Lafayette, Indiana 47907-1396

R.C. Shukla
Physics Department, Brock University, St. Catharines, Ontario, Canada L2S 3A1

(Received 29 September 1994)

Using high intensity ($\sim$ 70 Ci) ^{183}Ta Mössbauer sources, we have measured the elastic scattering fraction values, $\mathcal{F}$, and the relative integrated scattering intensities for the (200), (400), (600), and (220) Bragg planes of copper and silver single crystals; and for the (200), (400), and (600) reflections of a lead single crystal. The experiments were done as a function of temperature from 82 K to a high temperature of 1086, 1211, and 507 K for Cu, Ag, and Pb, respectively. The $\mathcal{F}$ values were found by Mössbauer line-shape studies, and were used to correct the measured integrated intensities for thermal-diffuse scattering, so that accurate Debye-Waller factors (DWF's) could be evaluated. The measured DWF's for Cu, Ag, and Pb each have a significant anharmonic contribution at about 50% of the melting temperature (T_m). Contrary to what Martin and O'Connor have reported for copper, we observed no Q^4 contribution to the DWF within our experimental errors, which we estimate to be smaller than those reported by Martin and O'Connor.

I. INTRODUCTION

The reduction of elastic scattering of photons by thermal motion of the atoms in a crystal is characterized by the Debye-Waller factor (DWF). It is a measure of the lattice-dynamical properties of a crystal. Its strong temperature dependence provides a method of understanding the anharmonic terms in interionic potentials used in calculations of lattice dynamics. However, the measurement of the Debye-Waller factor is complicated by thermal diffuse scattering (TDS), which is inelastic scattering due to lattice phonons. Because of the high-energy resolution of Mössbauer radiation ($\lesssim \mu$eV), Mössbauer γ-ray diffraction provides a method for experimentally separating the elastic and inelastic scattering. We have used this technique for studying the elastic scattering fraction and temperature dependence of the DWF for copper, silver, and lead single crystals, from which the contributions to the DWF, arising from anharmonic terms of the interatomic interaction potential, have been evaluated.

The resonant photons from the 46.5-keV ^{183}Ta Mössbauer source have an energy width of only 2.5 μeV, so that any phonon interaction upon scattering with the sample crystal will result in the scattered resonant photon's energy being shifted of order 10 meV, and cause it to appear as a 46.5-keV nonresonant photon, when analyzed with a Mössbauer absorber, whose Doppler-shifted spectrum detects only the zero phonon line. This lowers the observed resonance fraction, and gives us a measure of the crystal's elastic scattering fraction. The Mössbauer energy width is small enough that the probability of an incident nonresonant photon being inelastically scattered into an apparent resonant photon is negligible. Greater energy resolution is possible with other Mössbauer sources like ^{57}Co, which has an energy width of only 4.7 neV, but the ^{183}Ta sources can be fabricated with such superior photon intensity in the desired Mössbauer transition that it is much prefered for these DWF measurements, and its energy width is more than adequate to resolve the differences in energy due to phonon interactions.

Over the past 14 years many theoretical calculations of the atomic mean-square displacement and the Debye-Waller factor have been published for the fcc and bcc systems.[1–8] Two recent calculations are of interest from the view of comparison with theory and experiment. For Na and Kr, Shukla *et al.*[2,3] have shown that excellent agreement can be achieved between the lowest-order anharmonic perturbation theory (PT) and the DWF measured by Mössbauer techniques. For a comparison with the measurements presented in this paper, we have calculated the quasiharmonic (QH) terms, which include the standard harmonic and thermal expansion effect, and the PT contributions to the DWF for copper and silver.

In order to observe anharmonic effects, it is often necessary to make experimental measurements for higher-order Bragg reflections and at elevated temperatures. Under these experimental conditions, the TDS can be a substantial contribution to the total scattered intensity at a particular Bragg reflection and is a function of both temperature and reciprocal lattice vector. The TDS results from interactions between the incident photons and phonons present in the lattice, but the relative energy change ($\sim 10^{-2}$ eV) is so small that it is impossible to distinguish this from the elastically scattered Bragg component with standard x-ray techniques. The Mössbauer effect offers a method for experimentally separating the elastic and inelastic scattering components.

The separation of the elastic scattering from the inelastic may be achieved by using the high-energy resolution of the Mössbauer effect. This separation is cru-

0163-1829/95/52(1)/168(9)/$06.00

cial for the measurement of accurate DWF's, which only depend on the elastic scattering component. The high-intensity ($\sim$ 70 Ci) ^{183}Ta Mössbauer sources we are able to fabricate at the Missouri University Research Reactor (MURR) have two fundamental advantages over the typical 100 mCi ^{57}Co sources used in other experiments, namely, a factor of about 500 in the photon density for the desired Mössbauer transition, and a negligible source resonance self-absorption (SRSA) over the lifetime of the ^{183}Ta source, for once irradiated sources which were used in the present investigation. As was shown by Wagoner *et al.*,[9] the effect of SRSA can change the source recoilless fraction of a typical ^{57}Co source by more than 30% over its lifetime, and hence such measurements usually have a systematic error in the measurement of the elastic scattering over the time that the experiment is performed.

II. EXPERIMENTAL METHOD AND APPARATUS

By using the University of Missouri Research Reactor (MURR) facility, we have been able to fabricate and utilize exceptionally intense (70 Ci) ^{183}Ta sources and carry out precise Mössbauer effect studies with the 46.5-keV ^{183}W transition. The reactor at this facility produces a nominal flux of 3×10^{14} neutrons/(cm^2 s), which is considerably more intense than other university research reactors. The high neutron flux of this facility makes it possible to produce very intense ^{183}Ta sources, which are critical for doing accurate Mössbauer γ-ray diffraction experiments. Also, the reactor has a very short cycle time of 1 week, which is crucial in preparing the short half-life (5.1 days) source ^{183}Ta nearly free of the daughter ^{183}W, which gives unwanted SRSA.

The experiments on copper, silver, and lead have been carried out at MURR using the QUEGS (quasielastic gamma-ray scattering) instrument.[10] The QUEGS instrument consists of the following components: a stationary well-shielded source cask, a stage for crystal scattering which can accommodate a furnace or cryostat, a motor-driven oscillating platform for Doppler shifting Mössbauer absorbers, a solid-state photon detector, and a system of computer-controlled motors which control the crystal orientation and the scattering angle. The hand-crafted two-circle diffractometer allows computer control of θ and 2θ, with manual goniometer tilt settings of the sample crystals.

The typical distance between the source and detector is approximately 1.5 m. The beam is collimated upon exiting the source cask and also prior to entering the detector. The main collimator used in this experiment is a steel rectangular block about 60 cm from the source with a beam opening 2.54 cm high and 0.3 cm wide. A similar collimator is located just before the entrance of the detector.

For our experiments, the copper, silver, and lead sample crystals were fabricated by MR Semicon, Inc. The crystals were grown and cut perpendicular to the [h00] direction, so that the (h00) planes were parallel to the crystal face. After the final cut and polishing, the orientation of the crystals were verified by x-ray and neutron diffraction, and found to be accurate within 0.5°. According to the suppliers, the copper and silver crystals were 6N pure, and the lead crystal was 5N pure. All crystals had dimensions $3 \times 1 \times 0.1$ in. Even for the smallest Bragg angles at (200), the long crystals allowed the entire photon beam width to illuminate part of the crystal face and scatter in reflection, or Bragg, geometry. After all experiments, each crystal was checked by electron microscope measurements to check for possible contamination. It was found that there was not any contamination within 1% accuracy, and no heavy metal (iron, etc.) contamination to the precision of 0.2%.

Above room temperature, the crystals were heated by an electric furnace. The crystals were held by a C-shaped block of boron nitride with strips of soft quartz flax placed at the front edges in order to pack the crystal snug against the backing, and allow for sample expansion with temperature. Even at the highest temperatures, where temperature variation along the length of the crystal was maximum, the temperature uncertainty was less than 5 K. In order to avoid errors due to incidental bendings of the sample during temperature cycling, the rocking curves (ω scan) of the Bragg peaks were checked and found to be Gaussian at the various temperatures used in the experiment, and typical rocking curves are shown in Fig. 1. After all experiments, each crystal was checked by electron microscope measurements to check for possible contamination. It was found that there was no detectable contamination.

In order to measure the relative elastic scattering fraction $\mathcal{F}$, a resonant absorber of natural tungsten foil 2 mils thick was placed between the crystal and detector. The resonant absorber was Doppler shifted and a Mössbauer spectrum was generated for each Bragg plane and temperature studied. The recoilless fraction of the photon beam after crystal scattering was extracted by line-shape analysis for each Mössbauer spectrum.[11–15] Our line-shape studies used a full Mössbauer spectrum,

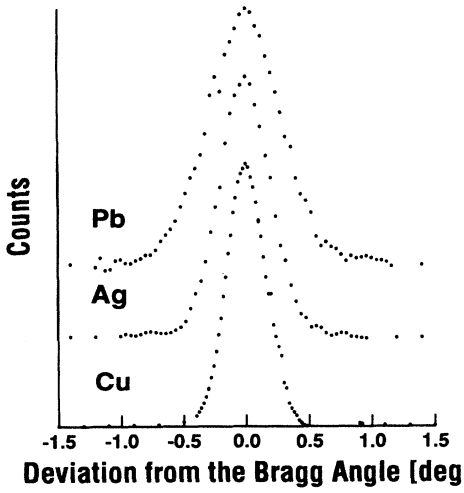

FIG. 1. The ω scan for the (200) Bragg plane of copper, silver, and lead at room temperature.

in contrast to the "on-off" method used in previous experiments, which only used two points to characterize a Mössbauer spectrum, one velocity at resonance and the other far from resonance. The "on-off" method also assumes that the Mössbauer dip scales linearly with the recoilless fraction of the photon beam, which is only true for an absorber with a thickness number much less than 1. Typical thickness numbers used are 3–4, where saturation effects are significant. Also, SRSA in ^{57}Co experiments changes in time, and this introduces a systematic error into "on-off" measurements.

By replacing the sample crystal by a LiF calibration crystal, the fraction of photons that were resonant before crystal scattering was found. For the (200) Bragg plane at room temperature, LiF is very nearly a 100% elastic scatterer of 46.5-keV γ rays,[16–18] and therefore a measurement of the photon beam resonance fraction is representative of the source resonance fraction. The relative elastic scattering fraction $\mathcal{F}$ was found from the ratio of the resonant photon fraction after crystal scattering, to before crystal scattering. The values of $\mathcal{F}$ were found as a function of Bragg plane and temperature. They were used to correct the integrated intensity measurements for inelastic scattering. Given the total scattering intensity for a particular reflection and temperature, the values of $\mathcal{F}$ were used to separate the elastic and inelastic scattering intensity contributions; i.e., $\mathcal{F}$ scales the total intensity measured under the rocking curve and yields the elastic intensity scattered by the crystal for any Bragg reflection.

III. THEORY

For imperfect (mosaic) crystals, the reduction of the Bragg intensity by atomic thermal vibrations is characterized by the Debye-Waller factor e^{-2M}. In a monatomic lattice with inversion symmetry, the exponential of the DWF may be written[19,20]

$$2M = Q^2\langle u_Q^2\rangle + \frac{1}{12}Q^4\left[3\langle u_Q^2\rangle^2 - \langle u_Q^4\rangle\right] + O(Q^6), \quad (1)$$

where $\vec{Q}$ is the scattering vector and $\langle u_Q^2\rangle$ is the atomic mean-squared deviation in the direction of $\vec{Q}$. For cubic crystals at high temperatures ($T > \Theta$), it may be written[6]

$$\langle u_Q^2\rangle = \frac{3\hbar}{Mk_B\Theta^2}T + m_2T^2 + m_3T^3 \quad (2)$$

and

$$\left[3\langle u_Q^2\rangle^2 - \langle u_Q^4\rangle\right] = m_4(hkl)\,T^3, \quad (3)$$

where M is the atomic mass, k_B is the Boltzmann constant, Θ is the Debye temperature, m_2 and m_3 are isotropic, anharmonic contributions due to the cubic and quartic terms in the crystal potential, which includes thermal expansion effects, and $m_4(hkl)$ is an anisotropic, anharmonic contribution which is also due to the cubic and quartic terms in the potential.

The anharmonic coefficients may be evaluated by fitting the measured Debye-Waller factors as a function of $\vec{Q}$ and T. In particular, the coefficient of the non-Gaussian term, $m_4(hkl)$, may be found directly by comparing the results for two sets of parallel Bragg planes defined by $\vec{Q}_1$ and $\vec{Q}_2$ ($\hat{Q}_1 = \hat{Q}_2$). Defining

$$\xi(T) \equiv \left[3\langle u_Q^2\rangle^2 - \langle u_Q^4\rangle\right]_T, \quad (4)$$

we have

$$\xi(T) - \xi(T_0) = \frac{12}{Q_1^2 - Q_2^2}\left\{\frac{1}{Q_1^2}\ln\left[\frac{E(\vec{Q}_1,T_0)}{E(\vec{Q}_1,T)}\right] - \frac{1}{Q_2^2}\ln\left[\frac{E(\vec{Q}_2,T_0)}{E(\vec{Q}_2,T)}\right]\right\}, \quad (5)$$

where

$$m_4(hkl) = \frac{\xi(T) - \xi(T_0)}{T^3 - T_0^3}. \quad (6)$$

Typically, the Debye-Waller factor is dominated by $\langle u_Q^2\rangle$ which contains isotropic terms in the exponential proportional to Q^2. The anharmonic coefficient $m_4(hkl)$ is a measure of the higher-order anisotropic, non-Gaussian term of the DWF.

In order to make a comparison between our experiment and theory we have carried our calculations of the DWF for copper and silver, where the interaction potentials can be calculated with reasonable confidence. For both materials we have used the experimental lattice spacings and a three-parameter Morse potential, whose parameters were determined by Shukla and MacDonald.[21] In addition, we have carried out the QH and PT calculations, also at the experimental lattice spacings for Cu, from a Born-Mayer potential. The parameters for the latter were determined by Cowley and Shukla,[22] where the Born-Mayer (BM) coefficient was determined at each volume and temperature. The condition used was that the compressibility determined from the slopes of the phonon dispersion curves be the same as that obtained from the total energy, which in addition to the BM term contained the Coulomb, exchange, and correlation energies, as well as a band structure term.

As can be seen in the subsequent discussion, this volume-dependent potential has a profound effect in the calculation of the DWF. In all our calculations a nearest-neighbor interaction was assumed for both potentials, and all Brillouin zone sums were evaluated in the limit that the step length from the origin to the boundary of the zone in the x direction tends to infinity. We emphasize this point because there is a disproportionate contribution from the points close to the origin.

IV. RESULTS AND DISCUSSION

Except for the (220) values of copper and silver, the temperature dependences for all Bragg planes of the sample crystals were done in ascending order. At each temperature, all Bragg planes were examined before rais-

ing the furnace temperature. For the copper and silver crystals, the (220) reflection was carried out after the temperature-dependent study of the (200), (400), and (600) Bragg planes. These latter measurements were done at reduced intensity, because we could not afford additional crystals cut perpendicular to the [$hh0$] or [hhh] directions.

Our integrated intensities were taken to be proportional to the peak values. The use of large single crystals in reflecting geometry gives an effective integrated intensity similar to that obtained by rotating a small crystal through the Bragg angle, provided that the incident beam intensity is spread over an angular divergence greater than the mosaic spread of the crystal. As a check, an ω scan was made for each Bragg plane and temperature. The sample crystal was rotated through the Bragg angle while the detector was kept fixed. At each temperature, a rocking curve was generated which provided a measure of the integrated intensities. The integrated intensities measured from the ω scans were proportional to the peak value measurements within errors for each sample crystal.

All of our rocking curves have a single peak of Gaussian line shape. They were each generated by an ω scan, which rotated the sample crystal through the Bragg angle by a system of computer-controlled motors with a step value of at least 0.02°, while the detector was kept fixed. Rocking curves of the (200) reflection at room temperature for copper, silver, and lead are shown in Fig. 1. The total integrated intensity was found by the area under the ω-scan peak. The rocking curve full width at half maximum for copper, silver, and lead were 0.369(3)°, 0.475(3)°, 0.678(3)°, respectively, and each were temperature independent. The collimation of our apparatus was such that the smallest rocking curve width that could be seen directly would have been about 0.2°.

Typical Mössbauer spectra are shown in Fig. 2 for the (220) reflection, as a function of temperature in the after configuration. A residual plot at the bottom indicates that the line-shape fitting correctly described the experimental data, and the reduced χ^2 values were between 1.0 and 1.1 for the data described in this paper.

The elastic scattering fraction values were derived from line-shape fits to our Mössbauer spectra, which were generated by scattering a beam of resonant 46.5-keV photons from the copper, silver, and lead sample crystals as a function of $\vec{Q}$ and T. The Mössbauer spectra for the (220) reflection of copper are shown in Fig. 2, which is representative of our spectra. Lead had the greatest change in elastic scattering fraction as a function of temperature. The elastic scattering fraction for lead was reduced by 7.7%, 28.0%, and 52.4% for the (200), (400), and (600) Bragg planes, respectively, for the temperature range of 82–507 K. Because of the very soft nature of lead and its low melting temperature, a relatively rapid falloff in the elastic scattering fraction with temperature is to be expected. Copper and silver have relatively stiffer lattices than lead and much higher melting points, and their corresponding elastic scattering fractions decrease with temperature much more slowly.

For silver, two crystals were used for experimentation.

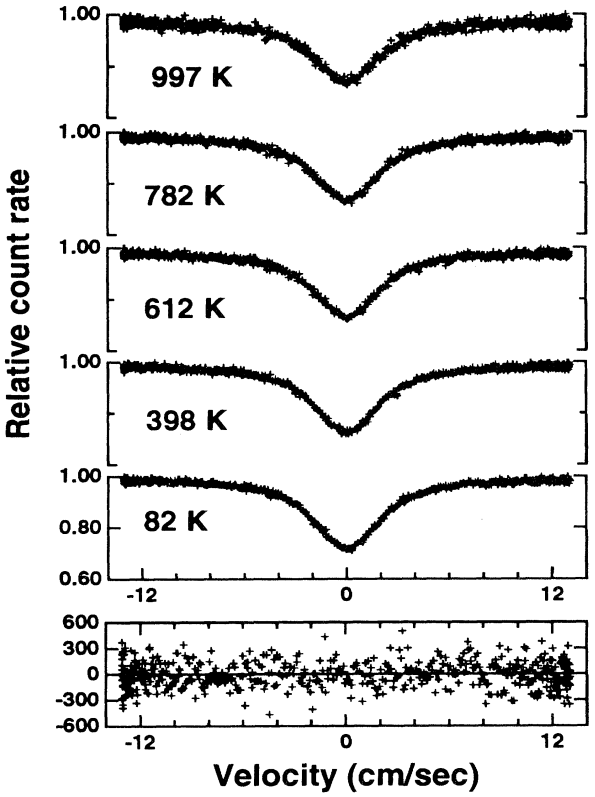

FIG. 2. Mössbauer spectra after scattering from the (220) Bragg plane of copper. The bottom figure is a residual plot for the 82 K spectrum.

The two are identical except that one has the [100] direction misoriented by 1.7° with respect to the crystal face. The silver data presented in this work were generated by γ-ray scattering from the accurately oriented crystal. The recoilless fractions measured with the "good" crystal and the misorientated one are the same within errors. This is to be expected, since the recoilless fraction or the elastic scattering fraction only depends on the sample temperature and scattering vector, and not on the relative scattering intensity, which is significantly reduced for the misoriented crystal. The equivalence of the elastic scattering fractions for the two silver crystals shows the reliability of measuring the elastic scattering fractions by the Mössbauer diffraction technique, and the possible small misorientations of the sample crystals are not a significant factor on the measured values. Our results for the elastic scattering fraction as a function of $\vec{Q}$ and T for copper, silver, and lead are plotted in Fig. 3. Using these results, we have obtained the elastic scattering intensities and their corresponding Debye-Waller factors, which are free from any TDS.

It is customary to report x-ray-integrated intensities by dividing out the Q^2 dependence. Therefore, our measured elastic integrated intensity values were converted into a more convenient form by means of the function

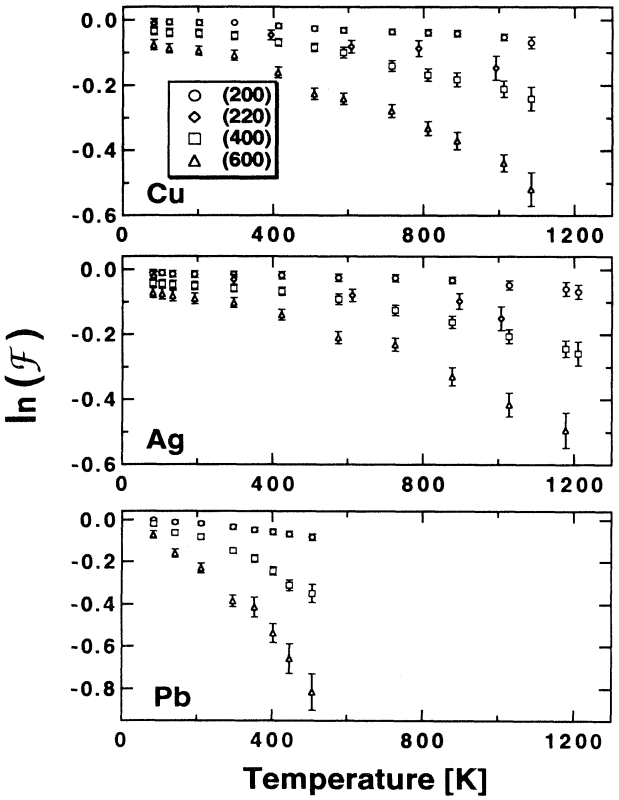

FIG. 3. Natural logarithm of the elastic scattering fraction values for copper, silver, and lead crystals vs. temperature.

$$Y(\vec{Q},T) \equiv \left(\frac{4\pi}{Q}\right)^2 \ln\left[\frac{E(\vec{Q},T)}{E(\vec{Q},T_0)}\right] = \left(\frac{4\pi}{Q}\right)^2 \left[2M(\vec{Q},T_0) - 2M(\vec{Q},T)\right], \quad (7)$$

for each reflection and temperature. Here $\vec{Q}$ is the scattering vector, $E(\vec{Q},T)$ is the measured elastic integrated intensity at temperature T, and T_0 is a reference at room temperature. This conversion made it easier to compare our data to previous results, or see any deviation from Q^2 in the exponent of the Debye-Waller factor which would imply a significant non-Gaussian contribution.

Using the above function, the measured elastic-integrated scattering intensities for copper, silver, and lead are plotted in Figs. 4, 5, and 6, respectively, along with the harmonic model and λ^2 theoretical calculations. Because of the complicated nature of the interatomic potential, an anharmonic theoretical calculation has not been attempted for lead. In its place, we have plotted the quasiharmonic model for lead, using 29.0 $\times$ 10^{-6}/K (Ref. 23) and 2.69 (Ref. 24) as values for the linear coefficient of thermal expansion and the Grünisen constant, respectively, at room temperature. This semiempirical approach gives a partial account of the anharmonicity as reflected in the thermal expansion.

As can be seen in Fig. 4, the Y data for copper lie

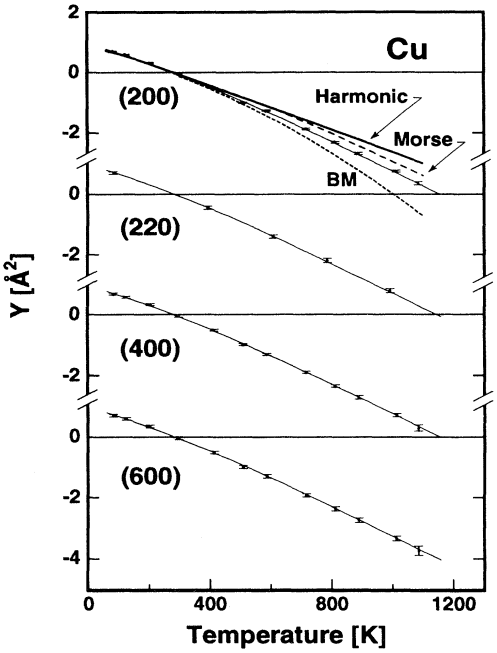

FIG. 4. A plot of $Y(\vec{Q},T)$ vs temperature for the copper crystal, and our theoretical calculations carried out with the Morse and BM potentials.

in between the Morse and BM anharmonic calculations. The copper data deviates significantly from the Morse model around 500 K and for the BM model around 700 K, which is about 40% and 50% of the melting temperature, respectively. At 1086 K, the average Y value for copper is 10% below the Morse calculation, and 23% above the

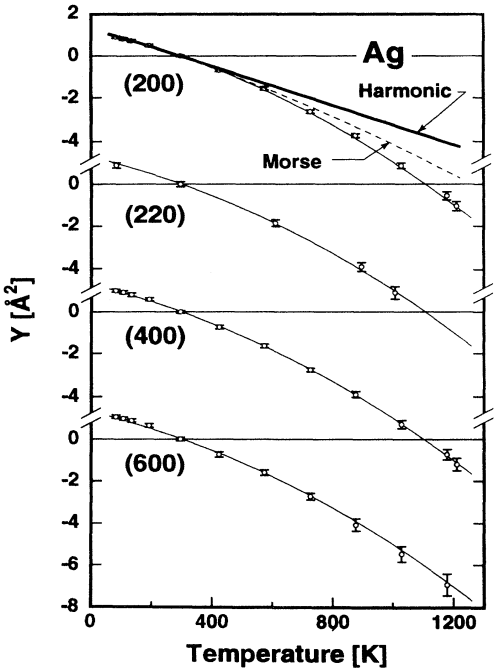

FIG. 5. A plot of $Y(\vec{Q},T)$ vs temperature for the silver crystal, and our theoretical calculations carried out with the Morse potential.

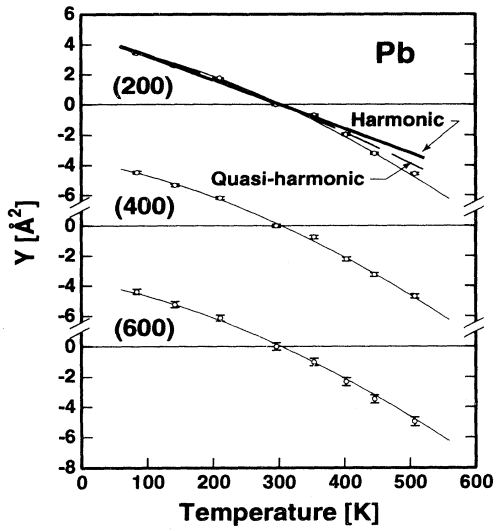

FIG. 6. A plot of $Y(\vec{Q},T)$ vs temperature for the lead crystal, with a quasiharmonic estimate of contributions to anharmonicity due to themal expansion.

BM calculation. As can be seen in Fig. 5, the silver Y data deviate significantly from the Morse model around 700 K which is about 60% of the melting temperature for Ag. At 1211 K, the average Y value for silver is 26% below the Morse calculation. The lead Y data, shown in Fig. 6, deviates significantly from the quasiharmonic model around 420 K, which is about 70% of the melting temperature for Pb. At 507 K, the average Y value for lead is 24% below the quasiharmonic model. For each metal crystal, there does not appear to be any significant non-Gaussian contribution to the Debye-Waller factor. If there were, there would be a visible separation in the Y data for the measurements at different Bragg planes because of its Q^4 dependence.

The Morse calculation of $2M$ for copper and silver, were both lower than our experimental data at high temperatures. The perturbation computation was carried out for 12 nearest neighbors, and the addition of more neighbors in the calculation did not bring the Morse model into better agreement with our experimental data for either copper or silver. Therefore, the disagreement between the Morse model and experiment is due to the limitation of the model itself. The BM model has a parameter which is a function of volume, and fits the copper data better than the Morse model, but instead of underestimating the anharmonicity like the Morse model, the BM model overestimates it at high temperatures. At temperatures about 50% of the melting temperature, the volume dependence of the two-body potential is significant and should not be ignored in the calculation of the Debye-Waller factor. So, for accurate calculations of the Debye-Waller factor for metal crystals, where the lattice expansion is large, the two-body atomic potential should allow for the volume-temperature dependence of the lattice.

The measured Debye temperatures for copper, silver, and lead are, respectively, 312(3), 214(4), and 83(10) K. These are all in good agreement with the values of 315, 215, and 88 K, respectively, reported for copper, silver, and lead by de Launay,[25] from specific heat data. All our measured parameters of the Debye-Waller factor are summarized in Table I.

The close agreement between our Mössbauer Debye temperatures and those determined from heat capacity data is surprising, and this agreement is probably due to the fact that the fcc crystals used in this study have simple dispersion curves, somewhat similar to an ideal Debye solid. Our Θ values for copper, silver, and lead are only a few percent less than those found from heat capacity measurements, and are, in fact, the same, within experimental errors. The reason that the difference is so small, even though the integrals for the heat capacity and Mössbauer recoilless fraction contain different weighting factors in ω, may be fortuitous, resulting from details of the true density-of-states dependence on ω. If we include one or two additional higher-temperature points in finding Θ from our data, these differences are greater, although the χ^2 values determined from fits to our data are also greater in this case.

The anharmonic parameters m_2 and m_3 were found by fitting our data to Eq. (1). For copper, a value of $m_2 = 4.1(1) \times 10^{-9}$ Å^2/K^2 was found, and no significant T^3 dependence was detected [$m_3 = 5(6) \times 10^{-13}$ Å^2/K^3]. The values $m_2 = 38(10) \times 10^{-10}$ Å^2/K^2 and $m_3 = 7.4(9) \times 10^{-12}$ Å^2/K^3 were found for silver, and $m_2 = 61(16) \times 10^{-9}$ Å^2/K^2 and $m_3 = 3.8(3) \times 10^{-11}$ Å^2/K^3 were returned for lead. A summary of our experimental results is given in Table I.

In our data, the exponential of the Debye-Waller factor for silver and lead both have a T^3 dependence, which is not observed for copper within our errors. This is most likely due to the nonlinear nature of the thermal lattice expansion at high temperatures. This idea is consistent with measured values for the thermal expansion of copper, silver, and lead.[26] Among the three metal crystals, lead has the greatest relative thermal lattice expansion and also the largest nonlinearity at high

TABLE I. Debye-Waller factor parameters.

Crystal	Θ [K]	m_2 [Å^2/K^2]	m_3 [Å^2/K^3]	$m_4(h00)$ [Å^4/K^3]
Cu	312(3)	$4.1(1) \times 10^{-9}$	$5(6) \times 10^{-13}$	$2(3) \times 10^{-13}$
Ag	214(4)	$38(10) \times 10^{-10}$	$7.4(9) \times 10^{-12}$	$1(2) \times 10^{-12}$
Pb	83(10)	$61(16) \times 10^{-9}$	$3.8(3) \times 10^{-11}$	$4(6) \times 10^{-12}$

temperatures ($T > 50\%\ T_m$), silver is next, and copper has the least relative thermal lattice expansion and the smallest nonlinearity. Our reported temperature dependence agrees with the results of Leadbetter,[27] where the measured Grünisen constants have a temperature dependence, which implies an effective temperature dependence for the Debye-Waller factors greater than the typical T^2 used in the quasiharmonic model.

The only similar experiment previously carried out on these metal crystals was done by Martin and O'Connor[28] for copper. In their paper, the most striking result was their claim to have observed the non-Gaussian term in Eq. (3). However, our experimental data for copper do not show evidence for such a term, and the theoretical calculations that we have carried out on the non-Gaussian term indicate that it is very small, and a factor of 10^{-4} smaller than the other more substantial Q^2 terms of the Debye-Waller factor.

In their experiment, Martin and O'Connor report a value of $m_2 = 7.7(6) \times 10^{-9}$ Å^2/K^2 for copper, which is 88% larger than our value. Much of the difference in the reported m_2 values appears to be caused by our different data refinement procedures. In their experiment, Martin and O'Connor allowed the Debye temperature to be a fitting parameter at the same time that m_2, m_3, and $m_4(hkl)$ were also fitting parameters for the high-temperature data. In our data analysis, the intent was to parametrize the harmonic approximation at low temperatures, for which the model was originally derived. In this way, the "true" anharmonic components could be found by their respective deviation from the harmonic model. Allowing the Debye temperature to be a free parameter at high temperatures changes the character of the harmonic approximation to a more quasiharmonic model. By letting the Debye temperature be a fitting parameter for our data, the returned value of the Debye temperature tends to be lower and the m_2 parameter moves slightly higher, into closer agreement with the reported value by Martin and O'Connor.

The criterion for fitting our low-temperature data of Y vs T to the harmonic approximation was to include only those data points which were within a standard error and not include higher-temperature data points, where the harmonic approximation is known to fail and where the deviation of the experimental and theoretical points is progressively greater than one standard error as the temperature increases.

The background corrections to the data are very important to the final results. The net effect of these background corrections is to bring our data into agreement with theory. If we do not make this correction, or if we obtain it improperly, our data for the exponent of the Debye-Waller factor will erroneously appear to contain a non-Gaussian (Q^4) component. For instance, if we fit the rocking curves with a Gaussian line shape to be used as a background correction for the total integrated intensity, and the resonant fraction values are not corrected for downscatter, the data falsely appear to contain a significant non-Gaussian component, because the rocking curves did not always fit exactly to a Gaussian line shape, and tended to give integrated intensity results which were as much as 5%, 7%, and 8% lower for copper, silver, and lead, respectively.

Using Eq. (6), we may easily see the pitfalls of this background correction. Figures 7(a) and 7(b) compare the results from the above background correction method (a), with the better and more complete approach (b), which uses the integrated counting rate in the multichannel scalar (MCS) window centered on the Bragg peak, and that of the MCS window centered to the left and right of the peak, and compares the counting rate for different radiation-heat-shield configurations used in the furnace at room temperature.

From a plot of Eq. (6) with their data, Martin and O'Connor[28] claim to observe a Q^4 dependence in the exponent of the Debye-Waller factor. The plot of Martin and O'Connor is very similar to our Fig. 7(a). Because the rocking curves do not always exactly fit a Gaussian line shape, the integrated intensities, which are taken to be proportional to the area under the curve, tend to be lower than they should be. This can lead to errors as high as 10% in the integrated intensities. The errors in the elastic integrated intensities can be even larger if their is significant downscatter in the Bragg peak, which would lower the recoilless fraction measurements, and correspondingly make the elastic integrated intensities even lower. Because of the sensitivity to the background correction, it is possible that Martin and O'Connor made an incorrect or incomplete correction, which resulted in an anomalous non-Gaussian term. We do not find any evidence for the non-Gaussian term in copper, silver, or lead.

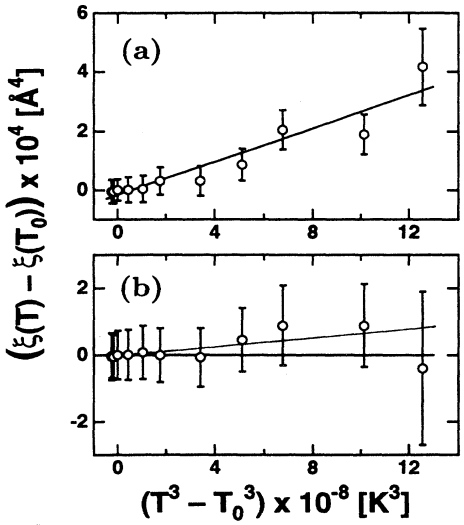

FIG. 7. A plot of the non-Gaussian (Q^4) contribution to the Debye-Waller factor for copper, which uses two different methods for correcting background. (a) only uses a background correction derived from a Gaussian line-shape fit to the rocking curves, and (b) applies corrections from the MCS-integrated counting rate, and furnace heat-shield downscatter. The slope corresponds to the $m_4(h00)$ coefficient.

V. CONCLUSION

The high-intensity ($\sim$ 70 Ci) ^{183}Ta Mössbauer sources we are able to fabricate at the University of Missouri Research Reactor allowed us to carry out precise Mössbauer γ-ray diffraction on copper, silver, and lead single crystals. These Mössbauer sources have two fundamental advantages over the typical 100 mCi ^{57}Co sources used in other experiments, namely, a factor of about 500 in the activity of the desired Mössbauer transition and a negligible source resonance self-absorption (SRSA) over the lifetime of the ^{183}Ta source. By this method, we have experimentally separated the elastic from the inelastic (thermal-diffuse) scattering, and have thus removed any systematic error from our measured integrated intensities. We have used this technique for studying the momentum transfer and temperature dependence of the Debye-Waller factor for copper, silver, and lead single crystals, from which the contributions to the Debye-Waller factor arising from anharmonic terms of the potential have been evaluated.

The Debye-Waller factor parameters Θ, m_2, and m_3, which were found by a fit of Eq. (1), are summarized in Table I. The additional Q^4 terms of Eq. (3), which is characterized by $m_4(hkl)$, were found to be $m_4(h00) = 2(3) \times 10^{-13}$ Å^4/K^3, $m_4(h00) = 1(2) \times 10^{-12}$ Å^4/K^3, and $m_4(h00) = 4(6) \times 10^{-12}$ Å^4/K^3 for copper, silver, and lead, respectively. Therefore, the quartic term is negligible to the accuracy of our experiment, which is more precise than any previous one.

Because the rocking curves do not always exactly fit a Gaussian line shape, the integrated intensities, which are taken to be proportional to the area under the curve, tend to be lower than they should. This can lead to errors as high as 10% in the integrated intensities. The errors in the elastic integrated intensities can be even larger if their is significant downscatter in the Bragg peak, which would lower the recoilless fraction measurements, and correspondingly make the elastic integrated intensities even lower. Because the Debye-Waller factors are sensitive to the background correction, it is possible that Martin and O'Connor made an incorrect or incomplete correction, which resulted in an aberrant non-Gaussian term. Contrary to what Martin and O'Connor[28] have reported for copper, we observed no significant Q^4 contribution to the Debye-Waller factor for copper, silver, or lead.

The Morse calculations of $2M$ for copper and silver were both lower than our experimental data at high temperatures. A perturbation computation by Shukla was carried out for 12 nearest neighbors, and the addition of more neighbors in the calculation did not bring the Morse model into better agreement with our experimental data for either copper or silver. Therefore, the disagreement between the Morse model and experiment is due to the limitation of the model itself. The BM model has a parameter which is a function of volume, and fits the copper data better than the Morse model, but instead of underestimating the anharmonicity like the Morse model, the BM model overestimates it at high temperatures. By comparing the Morse and BM models for copper, we can see how important it is to include the volume dependence for the potential. At temperatures about 50% of the melting temperature, the volume dependence of the two-body potential is significant and should not be ignored in the calculation of the Debye-Waller factor. This is consequential, because the Morse model is used by many researchers for calculating various solid-state properties of metal crystals (i.e., the elastic constants, bulk modulus, linear thermal expansion coefficient, and heat capacities, to name a few). So, for accurate high-temperature calculations of metal crystal properties, where the lattice expansion is large, the two-body atomic potential should allow for a volume-temperature dependence of the lattice.

In our data, the exponential of the Debye-Waller factor for silver and lead both have a T^3 dependence, which is not significantly observed for copper [$m_3 = 5(6) \times 10^{-13}$ Å^2/K^3]. This is most likely due to the nonlinear nature of the thermal lattice expansion at high temperatures. This idea is consistent with measured values for the thermal expansion of copper, silver, and lead.[26] For the three metals, lead has the greatest relative thermal lattice expansion and also the largest nonlinearity at high temperatures ($T > 50\%\ T_m$), silver is next, and copper has the least relative thermal lattice expansion and the smallest nonlinearity. Our reported temperature dependence agrees with the results of Leadbetter,[27] where the measured Grünisen constants have a temperature dependence, which implies an effective temperature dependence for the Debye-Waller factors greater than the typical T^2 used in the quasiharmonic model.

ACKNOWLEDGMENTS

This work was prepared with the support of the U.S. Department of Energy, Grant No. DE-FG02-85 ER 45199, and is taken from the Ph.D. thesis of John T. Day from Purdue University. We are appreciative of the MURR reactor facility and its personnel for its hospitality during the execution of this experiment. R.C.S. would like to acknowledge financial support from the Natural Sciences and Engineering Research Council of Canada (NSERC). Professor Guy Schupp gave technical assistance, which we wish to acknowledge.

[1] R. C. Shukla and D. W. Taylor, Phys. Rev. B **45**, 10 765 (1992).
[2] R. C. Shukla and D. W. Taylor, Phys. Rev. B **49**, 9966 (1994).
[3] R. C. Shukla and C. A. Plint, Phys. Rev. B **40**, 10 337 (1989).
[4] H. Hübschle and R. C. Shukla, Phys. Rev. B **40**, 11 920 (1989).

[5] R. C. Shukla and H. Hübschle, Solid. State Commun. **72**, 1135 (1989).
[6] G. A. Heiser, R. C. Shukla, and E. R. Cowley, Phys. Rev. B **33**, 2158 (1986).
[7] R. C. Shukla and R. D. Mountain, Phys. Rev. B **25**, 3649 (1982).
[8] R. C. Shukla and G. A. Heiser, Phys. Rev. B **33**, 2152 (1986).
[9] R. A. Wagoner, B. Bullard, M. May, S. Dickson, and J. G. Mullen, Hyperfine Interact. **58**, 2687 (1990).
[10] W. B. Yelon, G. Schupp, M. L. Crow, C. Holmes, and J. G. Mullen, Nucl. Instrum. Methods B **34**, 323 (1986).
[11] J. G. Mullen, A. Djedid, D. Cowan, G. Schupp, M. L. Crow, Y. Cao, and W. B. Yelon, Phys. Lett. **127**, 242 (1988).
[12] J. G. Mullen, A. Djedid, G. Schupp, D. Cowan, Y. Cao, M. L. Crow, and W. B. Yelon, Phys. Rev. B **37**, 3226 (1988).
[13] R. A. Wagoner, J. G. Mullen, and G. Schupp, Phys. Lett. B **279**, 25 (1992).
[14] B. Bullard, J. G. Mullen, and G. Schupp, Phys. Rev. B **43**, 7405 (1991).
[15] B. Bullard, J. G. Mullen, and G. Schupp, Phys. Rev. B **43**, 7416 (1991).
[16] J. G. Mullen and J. R. Stevenson, in *Workshop on New Directions in Mössbauer Spectroscopy*, edited by G. J. Perlow, AIP Conf. Proc. No. **38** (AIP, New York, 1977), p. 55.
[17] J. R. Stevenson, J. G. Mullen, and R. Colella, Nucl. Instrum. Methods. **164**, 125 (1979).
[18] J. G . Mullen, R. A. Wagoner, and G. Schupp, Hyperfine Interact. **83**, 147 (1994).
[19] G. A. Wolfe and B. Goodman, Phys. Rev. **178**, 1171 (1969).
[20] A. A. Maradudin and P. A. Flinn, Phys. Rev. **129**, 2529 (1963).
[21] R. C. Shukla and R. A. MacDonald, High Temp. High Press. **12**, 291 (1980).
[22] E. R. Cowley and R. C. Shukla, Phys. Rev. B **9**, 1261 (1974).
[23] R. C. Weast, *CRC Handbook of Chemistry & Physics*, 68th ed. (CRC Press, Boca Raton, 1988).
[24] E. W. Montroll, in *Handbook of Physics*, edited by E. U. Condon and H. Odishaw (McGraw-Hill, New York, 1958), pp. 5–155.
[25] J. de Launay, in *Solid State Physics*, edited by F. Seitz and D. Turnbull (Academic Press, New York, 1956), Vol. 2.
[26] Y. S. Touloukian, R. K. Kirby, R. E. Taylor, and P. D. Desai, *Thermal Expansion, Metallic Elements and Alloys*, edited by Y. S. Touloukian and C. Y. Ho (Plenum, New York, 1975), Vol. 12.
[27] A. J. Leadbetter, J. Phys. Chem. Solids **26**, 757 (1965).
[28] C. J. Martin and D. A. O'Connor, Acta Crystallogr. A **34**, 500 (1978); **34**, 505 (1978).